Eur. Phys. J. D **16**, 139–144 (2001)

THE EUROPEAN PHYSICAL JOURNAL D

EDP Sciences

Femtosecond surface plasmon resonance dynamics and electron-electron interactions in silver nanoparticles

C. Voisin, D. Christofilos, N. Del Fatti, and F. Vallée[a]

Laboratoire d'Optique Quantique du CNRS, École Polytechnique, 91128 Palaiseau Cedex, France

Received 1st December 2000

Abstract. Femtosecond excitation and relaxation of nonequilibrium electrons are investigated in silver clusters using a two color pump-probe technique with resonant excitation of the surface plasmon resonance and off resonant probing. The excitation process is shown to be identical to that in metal films, and permits creation of a strongly athermal single electron excitation in a time scale shorter than the duration of the pulses (25-30 fs), in agreement with the free-electron absorption model. Following the time evolution of the nonequilibrium distribution yields information on the internal energy redistribution dynamics of the conduction electrons and of its modification by confinement in metal clusters.

PACS. 78.47.+p Time-resolved optical spectroscopies and other ultrafast optical measurements in condensed matter – 42.65.-k Nonlinear optics

1 Introduction

With the advance of femtosecond lasers, the dynamic response of gas, liquid or solid media and, consequently, the elementary interaction mechanisms of their different degrees of freedom, can now be selectively studied using time-resolved techniques [1]. Of particular interest is the investigation of the size dependent dynamics of clusters that offer the unique possibility of following the change of the dynamic response of a material with its number of atoms, *i.e.*, the evolution from a solid to a few atom system. This problem has recently been addressed in the case of noble metals [2,3], and, in particular, modification of the internal electron energy redistribution dynamics by electron-electron scattering has been studied in bulk material and cluster down to a sizes of about 3 nm [4].

These investigations in metals are based on selective electron excitation on a time scale shorter than that of the electron-electron and/or electron-lattice thermalization times, the nonequilibrium electron relaxation being then followed by a probe pulse monitoring an electron distribution dependent property of the metal sample [2–9]. An important point here is the excitation process itself and how the femtosecond pump pulse interacts with the conduction electrons to create the initial athermal distribution. This is frequently described in terms of free electron absorption of the pump photon, considering only energy distribution and neglecting coherent processes. The aim of this paper is to give direct evidence of the validity of this approach in metal clusters when excitation is performed in resonance with the surface plasmon resonance, and to compare their response and the first steps of the energy redistribution processes to the ones in the bulk metal.

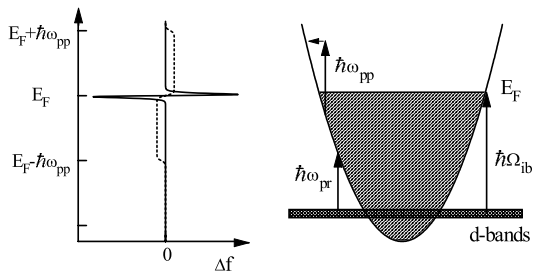

Fig. 1. Left: Energy dependence of the change of the electron occupation number Δf for a rise of the electron temperature (thermal distribution, full line) and for instantaneous intraband single electron excitation by a pump pulse of frequency ω_{pp} (athermal distribution). Right: Schematic electron band structure of noble metals. $\hbar\Omega_{ib}$ is the interband transition threshold between the top of the *d*-bands to the Fermi surface, with $\hbar\Omega_{ib} \approx 4$ eV in silver. The arrows indicate intraband electron excitation at $\hbar\omega_{pp}$ and off resonant probing at $\hbar\omega_{pr}$.

2 Femtosecond electron excitation

In our experiments in noble metals, we perturb the electron distribution by intraband absorption of a femtosecond pump pulse of frequency ω_{pp} (Fig. 1). The excitation frequency being far from the interband transitions ($\omega_{pp} < \Omega_{ib}$), energy is selectively injected in the conduction electrons without modification of their density.

[a] e-mail: vallee@leonardo.polytechnique.fr

During excitation, a coherent superposition of the electronic polarization and electromagnetic field of the pump pulse is initially created. This mixed material – field excitation has been described in bulk dielectric media using the polariton concept which is the eigenmode for light propagation [10]. Light absorption only takes place with polariton damping which usually reflects damping of the polariton material part. Similarly, metal excitation, *i.e.*, electron excitation, can be understood in terms of electron polarization decay. In bulk metal, this takes place due to electron-phonon and electron-electron scattering that lead to single electron excitation, and photon absorption can be globally interpreted as quasi-free electron absorption. In nanoparticles, for excitation in resonance with the surface plasmon resonance, the electron polarization is usually described in term of collective electron oscillation in a particle (*i.e.*, of coherent superposition of single electron modes) and, its decay discussed in terms of surface plasmon resonance dephasing. As discussed by Kawabata and Kubo, damping also takes place with single electron excitation, which is equivalent to Landau damping of the collective plasmon mode in a plasma [11].

In both bulk and confined metallic materials, this eventually leads to excitation of single electrons, each of them increasing its energy by $\hbar\omega_{pp}$. Electrons with an energy E between $E_F - \hbar\omega_{pp}$ and E_F are excited above the Fermi energy with a final energy between E_F and $E_F + \hbar\omega_{pp}$ (Fig. 1). Describing the conduction electrons by a one-particle distribution function f, the induced distribution change $\Delta f(E) = f(E) - f_0(E)$ is given by

$$\Delta f^{exc}(E) = B\{\sqrt{E-\hbar\omega_{pp}}\, f_0(E-\hbar\omega_{pp})[1-f_0(E)] - \sqrt{E+\hbar\omega_{pp}}\, f_0(E)[1-f_0(E+\hbar\omega_{pp})]\}, \quad (1)$$

where f_0 is the equilibrium electron distribution, B a pump intensity dependent parameter, and an isotropic parabolic conduction band has been assumed. Neglecting electron energy relaxation during the excitation process, the initial nonequilibrium electron distribution exhibits a step like shape as shown in Fig. 1.

Energy is subsequently redistributed among the electrons by electron-electron scattering, eventually leading to a hot Fermi distribution with temperature T_e on characteristic time scales of 350 fs in silver films [9]. During and after electron internal thermalization the injected energy is transferred to the lattice by electron-phonon interaction and electron-lattice thermalization is eventually reached in a few picoseconds (the characteristic electron-lattice energy exchange time is ~ 1 ps in noble metals).

The creation of this initial strongly athermal distribution can be directly followed by monitoring the optical property changes of the material far from the interband transition threshold. Conduction electron states well below E_F can then be monitored (Fig. 1), yielding information on their population change.

3 Optical response

The optical dielectric constant ϵ^{bulk} of a bulk metal at the frequency ω can be written as the sum of contributions of the conduction and bound electrons

$$\epsilon^{bulk}(\omega) = \epsilon^{f-bulk}(\omega) + \delta\epsilon^{b}(\omega). \quad (2)$$

In bulk noble metals, the main contribution to the bound electron term $\delta\epsilon^b(\omega) = \epsilon^b - 1$ is associated to the interband transitions from the fully occupied d-bands below the Fermi energy to the half filled s-p conduction band (Fig. 1). The conduction electrons follow a quasi-free electron behavior and their contribution ϵ^f to ϵ is well described by a Drude formula [12]

$$\epsilon^{f-bulk}(\omega) = 1 - \frac{\omega_p^2}{\omega[\omega + i/\tau_o^{bulk}(\omega)]}\ , \quad (3)$$

where ω_p is the plasma frequency ($\omega_p^2 = n_e e^2/\epsilon_0 m$, n_e and m being the conduction electron density and effective mass, respectively). $\tau_o^{bulk}(\omega)$ is the electron optical relaxation time which is determined by electron-phonon and electron-electron scattering with simultaneous exchange of a photon energy $\hbar\omega$ [13].

The quasi-free electron motion is modified in a nanocrystal due to electron interaction with the interface, and the concomitant breakdown of translational invariance. The intraband contribution to the dielectric constant of a metal cluster has been shown to keep a Drude-type form (3) [11,14], with the scattering time now being

$$\frac{1}{\tau^{cl}(\omega)} = \frac{1}{\tau_o^{cl}(\omega)} + \frac{v_F}{R} g_S(\omega)\ . \quad (4)$$

The first term, τ_o^{cl}, reflects the intrinsic bulk-like electron scattering processes in the particles. The second term, proportional to the Fermi velocity v_F divided by the radius R of the assumed spherical nanoparticle, is a consequence of the confinement of the electron motion. For not too small nanoparticles ($R \geq 1$ nm), modification of the interband transitions is negligible [15]. The total crystallite dielectric constant ϵ^{cl} thus takes a similar form as the bulk one (Eq. (2)) using the bulk $\delta\epsilon^b$ and replacing τ_o^{bulk} by τ^{cl} in (3).

In our experiments we are dealing with an ensemble of particles dispersed in a transparent dielectric matrix. For a low volume fraction $p \ll 1$ of small spheres ($R \ll \lambda$, where λ is the optical wavelength), the optical properties of this composite material can be described by introducing an effective dielectric constant $\widetilde{\epsilon}$ and its absorption coefficient can then be written [11,14]:

$$\widetilde{\alpha}(\omega) = \frac{9\, p\, \epsilon_d^{3/2}}{c} \frac{\omega\, \epsilon_2^{cl}(\omega)}{\left[\epsilon_1^{cl}(\omega) + 2\epsilon_d\right]^2 + \left[\epsilon_2^{cl}(\omega)\right]^2}, \quad (5)$$

where $\epsilon^{cl}(\omega) = \epsilon_1^{cl}(\omega) + i\epsilon_2^{cl}(\omega)$ and ϵ_d is the matrix dielectric constant. As compared to the bulk metal, the absorption is resonantly enhanced close to the frequency, Ω_R,

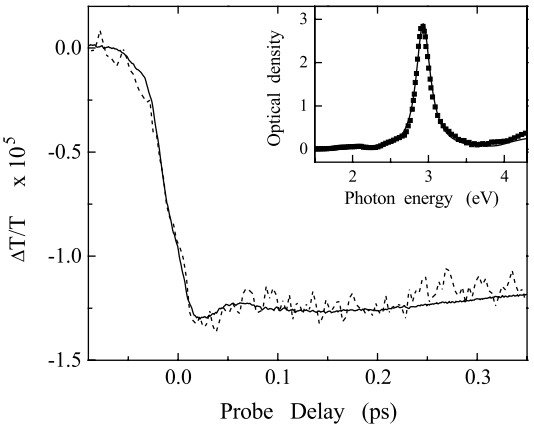

Fig. 2. Time dependence of the transmission change $\Delta T/T$ measured off resonance at $\hbar\omega_{pr} \approx 1.5$ eV for resonant excitation of the surface plasmon resonance $\hbar\omega_{pp} \approx \hbar\Omega_R \approx 3$ eV in $R = 13$ nm Ag nanoparticles in glass (full line). The dashed line is the normalized $\Delta T/T$ calculated from the measured $\Delta\epsilon_1^{bulk}(\omega_{pr})$ and $\Delta\epsilon_2^{bulk}(\omega_{pr})$ in a silver film using (8). The inset shows the measured sample absorption spectrum (squares) together with a fit (full line) using (5) with the bulk silver dielectric constant and including the surface term (Eq. (4), where g_S is used as a parameter).

minimizing the denominator which is the condition for the surface plasmon resonance (SPR) [11,14].

The absorption spectrum of silver nanoparticles with average radius $R = 13$ nm embedded in a glass (50BaO-50P_2O_5) matrix, is shown in the inset of Fig. 2. It is well reproduced using Eq. (5) with the measured bulk silver dielectric constant taking into account the additional surface term (Eq. (4), where g_S is used as a parameter). Conversely to other noble metals, the SPR is away from the interband transitions in silver ($\hbar\Omega_R \approx 3$ eV as compared to $\hbar\Omega_{ib} \approx 4$ eV). This is making silver a model material since the SPR or the interband transitions can be selectively excited or probed yielding selective information on the different electron interaction processes [3,4].

In time-resolved pump-probe experiments, the time dependent changes of the sample optical property (transmission, T, and/or reflectivity, R) induced by a pump pulse are monitored by a delayed probe pulse. These reflect alterations of the material dielectric function, $\Delta\epsilon(\omega_{pr})$, which are usually sufficiently weak to use a perturbational approach:

$$\frac{\Delta T(t_D)}{T} = \frac{\partial \ln T}{\partial \epsilon_1}\Delta\epsilon_1(t_D) + \frac{\partial \ln T}{\partial \epsilon_2}\Delta\epsilon_2(t_D) \quad (6)$$

$$\frac{\Delta R(t_D)}{T} = \frac{\partial \ln R}{\partial \epsilon_1}\Delta\epsilon_1(t_D) + \frac{\partial \ln R}{\partial \epsilon_2}\Delta\epsilon_2(t_D), \quad (7)$$

with $\epsilon = \epsilon^{bulk}$ in a metal film and $\epsilon = \widetilde{\epsilon}$ in a composite material. $\Delta T(t_D)$ ($\Delta R(t_D)$) is defined as the difference between the sample transmission (reflection) at time t_D minus the one without perturbation, at the probe frequency ω_{pr}. The coefficients of these linear combinations can be calculated from the material equilibrium optical response [3,9]. In metal film, $\Delta T(t_D)$ and $\Delta R(t_D)$ exhibit similar amplitudes permitting experimental determination of $\Delta\epsilon_1^{bulk}(t_D)$ and $\Delta\epsilon_2^{bulk}(t_D)$.

This cannot be done in dilute composite materials because of their small reflectivity and reflectivity changes (since $\widetilde{\epsilon}_1 \approx \epsilon_d$). In these systems, $\Delta T/T$ is only determined by $\Delta\widetilde{\epsilon}_2$, or, equivalently, by the sample absorption change [3,16]:

$$\frac{\Delta T}{T}(t_D) = -\Delta\widetilde{\alpha}(t_D)L = a_1\Delta\epsilon_1^{cl}(t_D) + a_2\Delta\epsilon_2^{cl}(t_D), \quad (8)$$

where L is the sample thickness. It is a linear combination of the changes of the real and imaginary parts of $\Delta\epsilon^{cl}(\omega_{pr})$. The coefficient a_1 and a_2 are related to the equilibrium $\epsilon^{cl}(\omega_{pr})$ (Eq. (5)) and are entirely determined after fitting the linear absorption spectrum [3]. The response in a metal film, assumed to be identical to a bulk material, can thus be compared to the one in nanoparticles by comparing the measured transmission change in the latter to the one calculated using the experimentally determined $\Delta\epsilon^{bulk}$ instead of $\Delta\epsilon^{cl}$ in (8).

4 Experimental setup

Excitation of silver nanoparticles in resonance with the SPR and probing out of resonance can be performed using the second harmonic and fundamental frequency of a Ti:sapphire laser, respectively. Our experimental system is based on a home-made femtosecond Ti:sapphire oscillator generating 25 fs frequency tunable near infrared pulses with an average power of 1 W at 80 MHz. Part of the pulse train is used as the probe beam in the near infrared ($\hbar\omega_{pr} \approx 1.5$ eV). The pump beam, close to the SPR frequency in silver nanoparticles ($\hbar\Omega_R \approx 3$ eV) was created by frequency doubling the remaining part in a 100 μm thick BBO crystal. After recompression in a fused silica prism pair the blue pulse duration, measured by cross-correlation of the IR probe and blue pump pulses, is about 30 fs with an average power of 20 mW. To resonantly probe the interband transitions in silver, femtosecond UV pulses can also be created by frequency tripling the pulse train [4,9].

A standard pump-probe setup has been used with mechanical chopping of the pump beam at 1.5 kHz and lock-in and differential detection of the probe beam transmission or reflection changes. The pump and probe beams were independently focused into the sample using fused silica lenses of 70 and 50 mm focal length, respectively. The high repetition rate (80 MHz) and stability of our femtosecond system permits noise levels for $\Delta T/T$ and $\Delta R/R$ measurements in the 10^{-6} range.

Measurements were performed in optically thin ($L =$ 23 nm) polycrystalline silver films and spherical silver nanoparticles embedded in a 50BaO-50P_2O_5 glass matrix. The latter samples were prepared by a fusion and heat treatment technique [17]. The metal volume fraction, p, is in the range 1×10^{-4}–5×10^{-4} with a sample thickness L of about 15 μm. The standard size deviation is smaller than 10 % of the average radius R.

5 Results and discussion

The temporal evolutions of the changes of the real and imaginary parts of the silver film dielectric constant, deduced from simultaneous $\Delta T/T$ and $\Delta R/R$ measurements are shown in Fig. 3a for $\hbar\omega_{pr} = 1.5$ eV and $\hbar\omega_{pp} = 3$ eV. $\Delta\epsilon_1^{bulk}$ is essentially determined by the changes of its interband part $\Delta\epsilon_1^b$, *i.e.*, that of the interband absorption spectrum induced by spreading of the electron distribution [9,18]. Using the Kramers-Kronig relationship, one can show that far from the interband transition threshold $\Delta\epsilon_1^b$ is weakly sensitive to the details of the electron distribution and almost follows energy injection and decay in the electron gas [18]. This is in agreement with the observed dynamics showing a fast rise and a slow decay due to electron energy losses to the lattice.

In contrast, $\Delta\epsilon_2^{bulk}$ is influenced by both the interband and intraband terms. The latter contribution is responsible for the long delay ($t_D > 50$ fs) signal that can be attributed to decrease of the electron scattering time τ_o^{bulk} (Eq. (3)). This response is consistent with our previous off-resonant study in silver (with $\hbar\omega_{pp} = \hbar\omega_{pr} \approx 1.5$ eV), showing in particular the same slow rise of $\Delta\epsilon_2^{bulk}$ up to $t_D \approx 100$ fs (Fig. 1) that reflects a delayed modification of the electron scattering rate [18]. On a shorter time scale, $\Delta\epsilon_2^{bulk}$ exhibits a fast rise and fall that can be ascribed to the interband term and is a signature of the large energy extension of the initial nonequilibrium distribution.

Interband absorption at ω_{pr} involves final conduction band states around $E_e = E_F - \hbar(\Omega_{ib} - \omega_{pr}) \approx E_F - 2.5$ eV, in the energy region where the electron occupation number is reduced by single electron excitation (from $E_F - \hbar\omega_{pp}$ to E_F, Fig. 1). Conduction band states are thus opened for interband absorption at ω_{pr} leading to an absorption increase that relaxes with population relaxation of these states, *i.e.*, in a few femtoseconds ($\sim$ 3 fs for electrons 2.5 eV above E_F [19], the "holes" below E_F having a similar dynamics as the corresponding electrons above E_F [9]). This leads to a transient increase of $\Delta\varepsilon_2^{bulk}$, whose temporal shape is essentially limited by the pump-probe cross-correlation. This interpretation is confirmed by the absence of a transient peak when exciting in the near infrared for the same probe frequency (Fig. 3b) no interband absorption being induced since the final states (with energy $\approx E_F - 2.5$ eV) are now unperturbed as they are 1 eV below the minimum energy of the perturbed states ($E_{min} = E_F - \hbar\omega_{pp} \approx E_F - 1.5$ eV).

The time dependence of the transmission change measured in silver nanoparticles with average radius $R = 13$ nm is shown in Fig. 2 for $\hbar\omega_{pr} = 1.5$ eV and $\hbar\omega_{pp} = 3$ eV, corresponding to resonant excitation of the nanoparticle surface plasmon resonance. The observed $\Delta T/T$ time behavior is, however, consistent with the one measured in a thin film with a small short time delay peak followed by a small $\Delta T/T$ increase over a 100 fs scale and a picosecond decay due to electron energy transfer to the lattice.

For the investigated nanoparticle size ($R = 13$ nm) the electron dynamics is almost identical to the bulk metal one [2,3], and the measured $\Delta T/T$ can be quantitatively compared to the bulk response using (8) and $\Delta\epsilon^{bulk}$

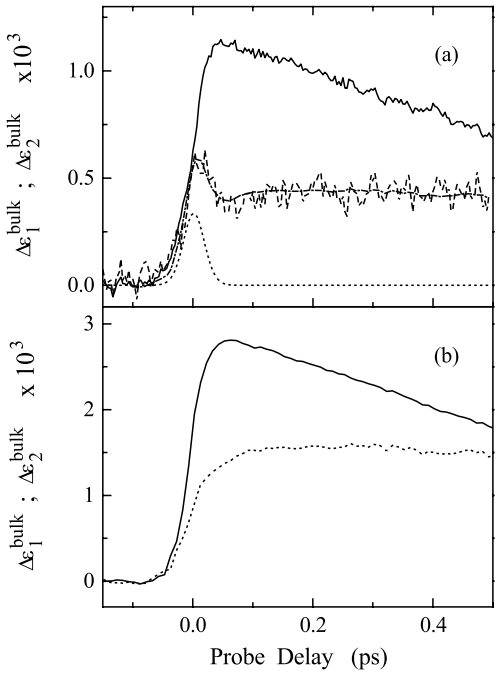

Fig. 3. (a) Measured time dependent changes of the real (full line) and imaginary (dashed line) parts of the dielectric function in a 23 nm Ag film at $\hbar\omega_{pr} \approx 1.5$ eV for $\hbar\omega_{pp} \approx 3$ eV. (b) Same as (a) for infrared excitation $\hbar\omega_{pp} = \hbar\omega_{pr} \approx 1.5$ eV [18]. The dotted line in (a) is the calculated change of the interband part of $\Delta\epsilon_2^{bulk}$ and the dash-dotted line its sum with $\Delta\epsilon_2^{f-bulk}$ measured for infrared pumping (b).

measured for the same pump and probe frequencies. A very good agreement between the experimental and calculated $\Delta T/T$ responses is obtained showing that the bulk and confined materials behave in a very similar way. For $\hbar\omega_{pr} = 1.5$ eV, the imaginary part of the metal dielectric constant yields an important contribution in nanoparticles ($a_2/a_1 \approx 2.7$ in (8)) and as for $\Delta\epsilon_2^{bulk}$, the transient interband induced absorption is actually at the origin of the observed $\Delta T/T$ transient peak. This shows that resonant SPR excitation in nanoparticles leads to the same single electron nonequilibrium distribution as non resonant excitation in films.

It is interesting to compare the measured response with the theoretical one assuming creation of a nonequilibrium distribution by direct single electron excitation by the pump pulse (*i.e.*, neglecting the coherent effects). In bulk materials, this can be done by first computing the electron distribution dynamics taking only energy redistribution processes into account, using the Boltzmann equation for the electrons:

$$\frac{df(E)}{dt} = \left.\frac{df(E)}{dt}\right|_{e-e} + \left.\frac{df(E)}{dt}\right|_{e-ph} + H(E,t), \qquad (9)$$

where $H(E,t) = AI_p(t)\Delta f^{exc}(E,t)$ stands for direct excitation by the pump pulse, $I_p(t)$ being the pump pulse intensity and A a constant setting the excitation amplitude (note that here f_0 has to be replaced by $f(t)$ in (1)). This approach has been used to model the electron

relaxation dynamics in bulk silver and we will use here the same electron-electron, $(df/dt)_{e-e}$, and electron-phonon $(df/dt)_{e-ph}$ scattering rates [9].

The change of the imaginary part of the interband term, $\Delta\epsilon_2^b(\omega_{pr})$, can thus be calculated using a model band structure for the d bands to conduction band transitions. As ω_{pr} is far from the interband transition threshold, the simple model of a parabolic conduction band and undispersed d-bands can be used [9]. The results are shown in Fig. 3 and, in agreement with the above qualitative discussion, $\Delta\epsilon_2^b(\omega_{pr})$ is found to be nonzero only for very short time delays. The second contribution to $\Delta\epsilon_2^{bulk}$, due to the intraband term, $\Delta\epsilon_2^{f-bulk}$, cannot be simply deduced from Δf and, as a first approximation, we have assumed that it is identical to the one measured for infrared pumping, ϵ_2^b being then unchanged (Fig. 3b). Summing this two terms, a very good description of the film data is obtained confirming that the observed transient peak is due to fast excitation of electrons out of states well below the Fermi energy (about 2.5 eV for $\hbar\omega_{pr} = 1.5$ eV). This good agreement also shows that coherent effects yield a negligible contribution to the measured response and that the electron excitation process can be simply described in term of single electron excitation (quasi-free electron absorption). This is also the case in metal nanoparticles, even for excitation of the surface plasmon resonance, the composite material response closely following the one deduced from the film study.

The absence of any detectable influence of coherent effects with the 25-30 fs pulses used here, is consistent with a fast polarization decay with the electron optical scattering time (*i.e.*, due to single electron scattering processes). This is of the order of 10 fs in bulk noble metals [12] and even smaller in nanoparticles because of the additional surface scattering contribution (Eq. (4)), in agreement with hole burning measurements [20] and time-resolved nonlinear investigations [21].

The further time evolution of the nonequilibrium electron distribution reflects electron energy redistribution processes, *i.e.*, the different electron scattering mechanisms. The fast decay of $\Delta\epsilon_2^b$ observed in films and clusters around $\hbar\omega_{pr} = 1.5$ eV reflects filling of the highly excited "holes" (Fig. 1) and thus the first steps in the evolution of the nonequilibrium electron distribution toward internal thermalization. This decay is accompanied by a large buildup of Δf around the Fermi energy (Fig. 1), and thus to a large change of the dielectric function for frequencies around Ω_{ib}. In contrast to the nonresonant probing situation discussed above, for probing around the interband threshold, $\omega_{pr} \approx \Omega_{ib} \approx 4$ eV, a slow rise of the transmission change is expected, reflecting this internal thermalization dynamics. This approach can be used in bulk and not too small clusters where the interband transition are not modified, and has been exploited to analyzed the impact of the confinement on electron-electron energy redistribution [4]. This is illustrated in Fig. 4 showing the transmission change $\Delta T/T$ measured at $\hbar\omega_{pr} = 3.95$ eV in $R = 13$ and 3 nm. The faster signal rise in the smaller nanoparticles clearly demonstrates acceleration of the electron-electron

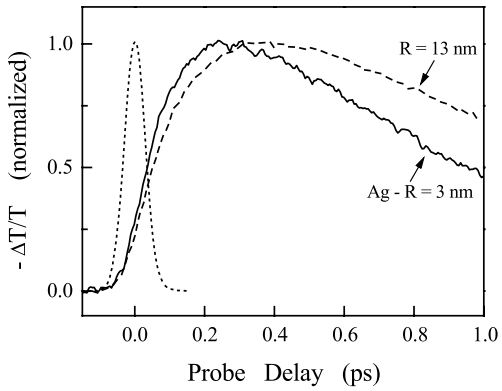

Fig. 4. Time behavior of the transmission change $-\Delta T/T$ measured in resonance with the interband transitions ($\hbar\omega_{pr} \approx$ 3.95 eV) for $\hbar\omega_{pp} \approx 1.32$ eV in $R = 13$ nm (dashed line) and 3 nm (full line) Ag nanoparticles in glass. The dotted line is the pump-probe cross-correlation.

energy exchanges in small nanoparticles as discussed in [4]. A characteristic thermalization time can then be defined from the $\Delta T/T$ rise, but one has to keep in mind that the distribution change around E_F is here mainly monitored (Fig. 1). This time is thus actually essentially determined by the electron-electron scattering processes around the Fermi surface whose probabilities are largely reduced by the Pauli exclusion principle effects and are the slowest mechanisms involved in the internal thermalization [9].

6 Conclusion

Using a two-color femtosecond pump-probe technique, we have investigated ultrafast creation and relaxation of a nonequilibrium electron distribution in silver nanoparticles for resonant excitation of the surface plasmon resonance. Probing far from the interband transition threshold, it is possible to follow the transient occupation number of electron states well below the Fermi energy (about 2.5 eV). This is found to be reduced in a time scale shorter than our time resolution yielding evidence for ultrafast excitation of low energy electrons and, thus, perturbation of the distribution over a very broad energy range, in agreement with the single electron damping model of the surface plasmon resonance (Landau damping). These results are in very good agreement with those obtained in metal film for the same pump and probe conditions and with numerical simulation of the electron dynamics. This shows that the model of free-electron absorption of the pump photon can be used to described femtosecond electron excitation in bulk and confined metallic materials, neglecting coherent effects. Ultrafast energy redistribution among the electrons and toward the lattice can thus be followed, yielding information on electron interaction processes in metals [2–4]. Extension of these investigations to small metal clusters and application of other time resolved techniques, such as time-resolved two-photon photoemission [19,22], to their study would be particularly interesting.

The authors wish to acknowledge B. Prével, M. Gaudry, E. Cottancin, J. Lermé, M. Pellarin, and M. Broyer for their help in the theoretical and experimental parts of this work, and A. Nakamura, Y. Hamanaka, S. Omi for helpful discussions and for providing the silver nanoparticle samples.

References

1. See for instance: *Ultrafast Phenomena XI*, edited by T. Elsaesser, J.G. Fujimoto, D.A. Wiersma, W. Zinth (Springer Verlag, Berlin, 1998).
2. S. Link, M.A. El-Sayed, J. Phys. Chem. B **103**, 8410 (1999).
3. C. Voisin, N. Del Fatti, D. Christofilos, F. Vallée, J. Phys. Chem. B **105**, 2264 (2001).
4. C. Voisin, D. Christofilos, N. Del Fatti, F. Vallée, B. Prével, E. Cottancin, J. Lermé, M. Pellarin, M. Broyer, Phys. Rev. Lett. **85**, 2200 (2000).
5. H.E. Elsayed-Ali, T.B. Norris, M.A. Pessot, G.A. Mourou, Phys. Rev. Lett. **58**, 1212 (1987).
6. R.W. Schoenlein, W.Z. Lin, J.G. Fujimoto, G.L. Eesley, Phys. Rev. Lett. **58**, 1680 (1987).
7. C.K. Sun, F. Vallée, L.H. Acioli, E.P. Ippen, J.G. Fujimoto, Phys. Rev. B **50**, 15337 (1994).
8. R. Groeneveld, R. Sprik, A. Lagendijk, Phys. Rev. B **51**, 11433 (1995).
9. N. Del Fatti, C. Voisin, M. Achermann, S. Tzortzakis, D. Christofilos, F. Vallée, Phys. Rev. B **61**, 16956 (2000).
10. D.L. Mills, E. Burstein, Rep. Prog. Phys. **37**, 817 (1974).
11. A. Kawabata, R. Kubo, J. Phys. Soc. Jap. **21**, 1765 (1966).
12. P.B. Johnson, R.W. Christy, Phys. Rev. B **6**, 4370 (1972).
13. J.B. Smith, H. Ehrenreich, Phys. Rev. B **25**, 923 (1982).
14. U. Kreibig, M. Vollmer, *Optical Properties of Metal Clusters* (Springer, Berlin, 1995).
15. U. Kreibig, *Handbook of Optical Properties*, edited by R.E. Hummel, P. Wissmann (CRC Press, New York, 1997), Vol. 2, p. 145.
16. N. Del Fatti, F. Vallée, C. Flytzanis, Y. Hamanaka, A. Nakamura, Chem. Phys. **251**, 215 (2000).
17. K. Uchida, S. Kaneko, S. Omi, C. Hata, H. Tanji, Y. Asahara, A.J. Ikushima, T. Tokisaki, A. Nakamura, J. Opt. Soc. Am. B **11**, 1236 (1994).
18. N. Del Fatti, R. Bouffanais, F. Vallée, C. Flytzanis, Phys. Rev. Lett. **81**, 922 (1998).
19. M. Aeschlimann, M. Bauer, S. Pawlik, Chem. Phys. **205**, 127 (1996).
20. F. Stietz, J. Bosbach, T. Wenzel, T. Vartanyan, A. Goldmann, F. Träger, Phys. Rev. Lett. **84**, 5644 (2000).
21. B. Lamprecht, A. Leitner, F.R. Aussenegg, Appl. Phys. B **68**, 419 (1999).
22. M. Fierz, K. Siegmann, M. Scharte, M. Aeschlimann, Appl. Phys. B **68**, 415 (1999).